

Analysis of anomalous traps measured by charge pumping technique in HfO₂/metal gate n-channel metal-oxide-semiconductor field-effect transistors

Szu-Han Ho, Ting-Chang Chang, Ying-shin Lu, Wen-Hung Lo, Ching-En Chen, Jyun-Yu Tsai, Hua-Mao Chen, Chi-Wei Wu, Hung-Ping Luo, Guan-Ru Liu, Tseung-Yuen Tseng, Osbert Cheng, Cheng-Tung Huang, and Simon M. Sze

Citation: *Applied Physics Letters* **101**, 233509 (2012); doi: 10.1063/1.4769444

View online: <http://dx.doi.org/10.1063/1.4769444>

View Table of Contents: <http://scitation.aip.org/content/aip/journal/apl/101/23?ver=pdfcov>

Published by the *AIP Publishing*

Articles you may be interested in

Investigation of abnormal negative threshold voltage shift under positive bias stress in input/output n-channel metal-oxide-semiconductor field-effect transistors with TiN/HfO₂ structure using fast I-V measurement

Appl. Phys. Lett. **104**, 113503 (2014); 10.1063/1.4868532

Investigation of extra traps measured by charge pumping technique in high voltage zone in p-channel metal-oxide-semiconductor field-effect transistors with HfO₂/metal gate stacks

Appl. Phys. Lett. **102**, 012106 (2013); 10.1063/1.4773914

Investigation of an anomalous hump in gate current after negative-bias temperature-instability in HfO₂/metal gate p-channel metal-oxide-semiconductor field-effect transistors

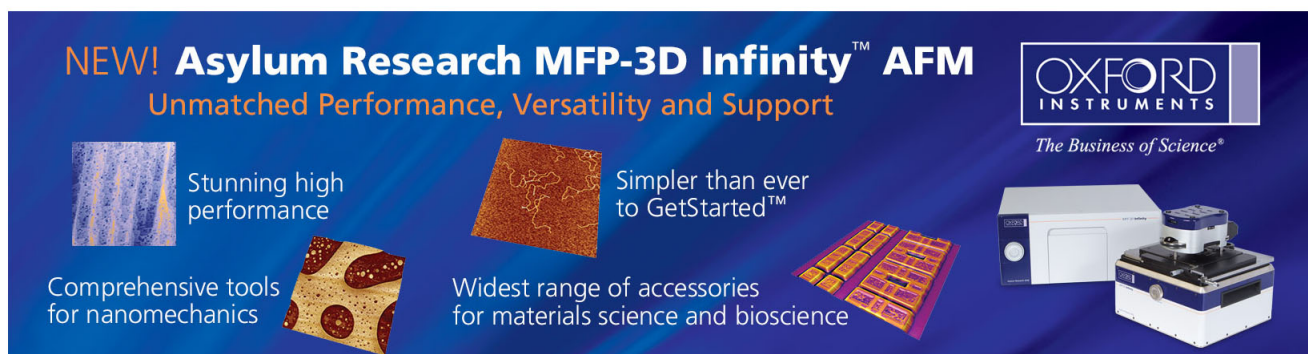
Appl. Phys. Lett. **102**, 012103 (2013); 10.1063/1.4773479

Analysis of an anomalous hump in gate current after dynamic negative bias stress in Hf_xZr_{1-x}O₂/metal gate p-channel metal-oxide-semiconductor field-effect transistors

Appl. Phys. Lett. **101**, 052105 (2012); 10.1063/1.4739525

Anomalous negative bias temperature instability behavior in p-channel metal-oxide-semiconductor field-effect transistors with Hf Si O N Si O₂ gate stack

Appl. Phys. Lett. **90**, 233505 (2007); 10.1063/1.2745649



NEW! Asylum Research MFP-3D Infinity™ AFM
Unmatched Performance, Versatility and Support

OXFORD INSTRUMENTS
The Business of Science®

Stunning high performance
Simpler than ever to GetStarted™
Comprehensive tools for nanomechanics
Widest range of accessories for materials science and bioscience

The advertisement features several images: a blue textured surface, a brown textured surface, a yellow and red patterned surface, a set of colorful rectangular samples, and the Asylum Research MFP-3D Infinity AFM instrument.

Analysis of anomalous traps measured by charge pumping technique in HfO₂/metal gate n-channel metal-oxide-semiconductor field-effect transistors

Szu-Han Ho,¹ Ting-Chang Chang,^{1,2,a)} Ying-shin Lu,² Wen-Hung Lo,² Ching-En Chen,¹ Jyun-Yu Tsai,² Hua-Mao Chen,³ Chi-Wei Wu,¹ Hung-Ping Luo,¹ Guan-Ru Liu,² Tseung-Yuen Tseng,¹ Osbert Cheng,⁴ Cheng-Tung Huang,⁴ and Simon M. Sze^{1,2,5}

¹Department of Electronics Engineering, National Chiao Tung University, Hsinchu 300, Taiwan

²Department of Physics, National Sun Yat-Sen University, Kaohsiung 804, Taiwan

³Department of Photonics & Institute of Electro-Optical Engineering, National Chiao Tung University, Hsinchu, Taiwan

⁴Device Department, United Microelectronics Corporation, Tainan Science Park, Taiwan

⁵Department of Electronics Engineering, Stanford University, Stanford, California 94305, USA

(Received 20 September 2012; accepted 16 November 2012; published online 7 December 2012)

This letter investigates anomalous traps measured by charge pumping technique in high voltage in HfO₂/metal gate n-channel metal-oxide-semiconductor field-effect transistors. N-V_{high level} characteristic curves with different duty ratios indicate that the electron discharge time dominates the value of N for extra traps. By fitting $\ln(N(t_{\text{base level}} = 2.5 \mu\text{s}) - N(t_{\text{base level}})) - \Delta t_{\text{base level}}$ at different temperatures and computing the equation $t = \tau_0 \exp(\alpha_{\text{e,SiO}_2} d_{\text{SiO}_2} + \alpha_{\text{e,HfO}_2} d_{\text{HfO}_2, \text{trap}})$, results show that these extra traps measured by the charge pumping technique at high voltage can be attributed to high-k bulk shallow traps. © 2012 American Institute of Physics.

[<http://dx.doi.org/10.1063/1.4769444>]

With the scaling down of metal-oxide semiconductor field-effect transistors (MOSFETs), conventional SiO₂-based dielectric is only a few atomic layers thick, causing gate current to rise, power dissipation to increase, and performance to degrade. In addition, conventional SiO₂-based dielectrics have approached their physical limits. Consequently, replacing SiO₂-based dielectrics with high-k based dielectrics is a valid solution to these problems. Furthermore, high-k/metal gates can be integrated with techniques such as silicon on insulator (SOI),¹⁻³ strained-silicon,^{4,5} and multi-gate to improve device characteristics. As recommended in the International Technology Roadmap for Semiconductors, Hf-based dielectrics have been heavily studied to replace SiO₂-based dielectrics in recent years.⁶⁻⁹ However, with changes in Hf-based dielectrics, many measurement techniques must be corrected, especially charge pumping techniques. For instance, with a decrease in frequency, charge pumping current (I_{cp}) decreases in conventional SiO₂-based dielectrics since carriers have enough time to discharge from interface shallow traps. Conversely, with a decrease in frequency, I_{cp} increases in Hf-based dielectrics since carriers have enough time to tunnel into high-k bulk traps.¹⁰ Charge pumping techniques play an important role to inspect defect. Thus, this study mainly focuses on anomalous traps measured by the charge pumping technique at high voltage, with the devices used in this study HfO₂ dielectrics n-MOSFETs. The causes of the anomalous traps are explained in this letter.

The HfO₂/metal gate n-MOSFETs used in this study were fabricated by the gate first process. First, a high quality 1 nm-thick thermal oxide was grown as an interfacial layer. Second, 3 nm of HfO₂ dielectrics were sequentially deposited by atomic layer deposition. Third, 10 nm of Ti_xN_{1-x} was

deposited by radio frequency physical vapor deposition, because metal gates can eliminate gate depletion and resist remote phonon scattering.^{11,12} Next, poly-Si was deposited as a low resistance gate electrode. Finally, the dopant activation was performed at 1025 °C. The n-MOSFETs are measured by the charge pumping technique with different duty ratios at different temperatures. A pulse train with low-voltage of -0.6 V, high-voltage from 0 V to 1.8 V, and frequency of 200 kHz was applied on the gate terminal. I_g-V_g transfer curves were measured with the source, drain, and body terminals all grounded, with V_g given from 0 V to 1.8 V. Then through body floating (BF), source/drain floating (SDF), and source/drain/body all grounded (SDB) process, the current path and carrier polarity can be confirmed. Next, the I_g-V_g curve is fitted by Frenkel-Poole current and tunneling current. All experimental curves were measured using an Agilent B1500 semiconductor parameter analyzer.

Figure 1 shows the N-V_{high level} characteristic curves at different duty ratios. N is the number of traps, and duty ratio = (t_{high level}/t_{cycle}). Clearly, N-V_{high level} characteristic curves are the same in the V_{high level} < 1.1 V with an increase in duty ratio. This information implies that interface traps detected by the charge pumping technique are not dependent on t_{base level}. This is because the time for electrons in the interface traps to recombine with holes is very short. Hence, the numbers of interface traps measured by I_{cp} are not sensitive to duty ratio. On the contrary, N decreases with a rise in duty ratio in V_{high level} > 1.1 V. Furthermore, only interface traps can be measured with a duty ratio value of 98%. In other words, extra traps nearly disappear. The detrapping time (t_{base level}) of electron dominates the value of N such that N becomes smaller with a decrease in detrapping time. This demonstrates that electrons need time to discharge. Thus, it is necessary to know the relationship between N and the detrapping time (t_{base level}) in V_{high level} > 1.1 V. The inset of the Fig. 1

^{a)}Electronic mail: tcchang@mail.phys.nsysu.edu.tw.

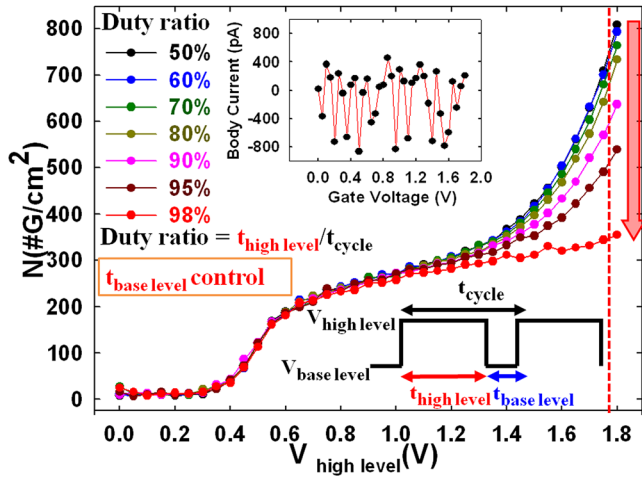


FIG. 1. N - $V_{\text{high level}}$ characteristic curves at different duty ratios by charge pumping measurement. Inset shows $I_{\text{sub}}-V_g$ curve with source, drain, and body all grounded.

shows $I_{\text{sub}}-V_g$ curves with source, drain, and body all grounded. It can be first observed that body current is small. In addition, $N(I_{\text{cp}})$ is dependent on the detrapp time. Hence, these results mean that N measured by the charge pumping technique is not caused by gate leakage current, but rather high- k bulk traps that have been detected, as shown in the energy band diagram of Fig. 2.

The inset of Figure 2 shows $N-t_{\text{base level}}$ curve at 30°C , for $V_g = V_t (0.67\text{ V}) + 1.1\text{ V}$, as shown by the dotted red line in Fig. 1. Since N can also represent the numbers of electrons discharged from high- k bulk traps, $N(t_{\text{base level}} = 2.5\mu\text{s}) - N(t_{\text{base level}})$ is the number of electrons still charged in the high- k bulk traps at $t_{\text{base level}}$, an important parameter. Figure 2 shows $\ln(N(t_{\text{base level}} = 2.5\mu\text{s}) - N(t_{\text{base level}})) - \Delta t_{\text{base level}}$ curves fitted from the inset of Figure 2. $\Delta t_{\text{base level}}$ is $t_{\text{base level}} - t_{\text{base level}}$ ($0.1\mu\text{s}$). $\Delta t_{\text{base level}}$ is the time for electrons to discharge from traps. Clearly, fitting these curves can be accomplished with straight lines even for different temperatures. In addition, slopes are also similar at these temperatures. The

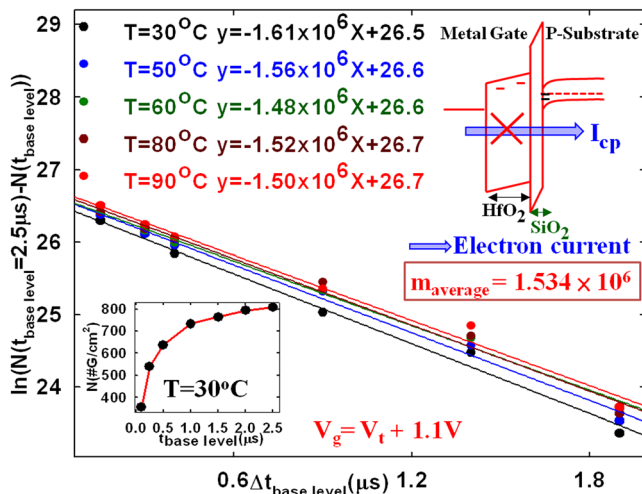


FIG. 2. $\ln(N(t_{\text{base level}} = 2.5\mu\text{s}) - N(t_{\text{base level}})) - \Delta t_{\text{base level}}$ curves at different temperatures at $V_g = V_t + 1.1\text{ V}$. Inset shows $N-t_{\text{base level}}$ curve in 30°C at $V_g = V_t (0.67\text{ V}) + 1.1\text{ V}$. The energy band diagram shows I_{cp} is caused by bulk trap, not gate leakage current.

discharge equation can be described by $dQ(t)/dt = -\Delta Q(t)/\tau_p = -e_p \Delta Q(t)$, $\Delta Q(t) = \Delta Q(0)\exp(-e_p t)$,¹³ where e_p is the escape probability and τ_p is the average escape time. Thus, slope is indicated by e_p or $1/\tau_p$ with e_p not dependent on temperature. Hence, e_p may be the tunneling probability. The average value of the slope at different temperatures (m_{average}) is 1.534×10^6 , and $\tau_{p,\text{average}}$ is $6.52 \times 10^{-7}(\text{s})$. Now the value of tunneling distance can be determined by using $\tau_{p,\text{average}}$ and can verify that the traps are actually in the high- k bulk. The relationship between tunneling time and distance can be approximated by $t = \tau_0 \exp(\alpha_e x)$, $\alpha_e = 2(2m_e q\phi_0/\hbar^2)^{0.5}$,^{14,15} where τ_0 is an electron tunneling characteristic time, m_e is electron effective mass for SiO_2 , and $q\phi_0$ is an effective tunneling barrier height. However, because electrons are tunneling through two layers, SiO_2 and HfO_2 , this equation can be described by $t = \tau_0 \exp(\alpha_{e,\text{SiO}_2} d_{\text{SiO}_2} + \alpha_{e,\text{HfO}_2} d_{\text{HfO}_2,\text{trap}})$, $\alpha_{e,\text{SiO}_2} = 2(2m_{e,\text{SiO}_2} q\phi_{0,\text{SiO}_2}/\hbar^2)^{0.5}$, and $\alpha_{e,\text{HfO}_2} = 2(2m_{e,\text{HfO}_2} q\phi_{0,\text{HfO}_2}/\hbar^2)^{0.5}$, where d_{SiO_2} is the thickness of SiO_2 , $d_{\text{HfO}_2,\text{trap}}$ is the distance from traps to interlayer between SiO_2 and HfO_2 , m_{e,SiO_2} and m_{e,HfO_2} are effective mass in SiO_2 and HfO_2 , respectively, and $q\phi_{0,\text{SiO}_2}$ and $q\phi_{0,\text{HfO}_2}$ are effective tunneling barrier height in SiO_2 and HfO_2 , respectively. τ_0 , m_{e,SiO_2} , and m_{e,HfO_2} can be obtained from other research.^{14,16,17} Thus, only one parameter (ϕ_{0,HfO_2}) is unknown.

The inset in Figure 3(a) shows I_g-V_g characteristic curves with BF, SDF, and SDB for distinguishing gate current at 30°C . Clearly, the I_g-V_g characteristic curve in BF is similar to that in SDB, and the I_g-V_g characteristic curve in SDF is much smaller than either. These results indicate that electrons transfer from source/drain to the gate, rather than holes transferring from gate to body. Clearly, section A indicates the tunneling current in Fig. 3(b), from $V_g = 0.35\text{ V}$ to $V_g = 0.75\text{ V}$, while section B is Frenkel-Poole current, shown in the inset of Fig. 3(d), from $V_g = 1.1\text{ V}$ to $V_g = 1.8\text{ V}$. $\varphi_B = 0.49\text{ eV}$ can be obtained by fitting the Frenkel-Poole mechanism in the inset in Fig. 3(d).¹⁸⁻²⁰ Figure 3(c) shows the $N-V_{\text{high level}}$ characteristic curves at different duty ratios. It can be observed that when $V_g < 1.1\text{ V}$, N is interface traps (N_{it}) only. On the contrary, when $V_g > 1.1\text{ V}$, N is both high- k bulk shallow traps (N_{hkst}) and N_{it} . A comparison of Fig. 3(c) with Fig. 3(a) shows that N is only N_{it} when gate current is tunneling current and Frenkel-Poole current is very small. Conversely, N is both N_{it} and N_{hkst} when gate current is Frenkel-Poole current. This indicates that bulk traps charging electrons via the Frenkel-Poole mechanism and the traps discharging electrons through I_{cp} may be the same. In order to confirm this theory, $\varphi_B = \phi_{0,\text{HfO}_2} = 0.49\text{ eV}$ is substituted into the equation $t = \tau_0 \exp(\alpha_{e,\text{SiO}_2} d_{\text{SiO}_2} + \alpha_{e,\text{HfO}_2} d_{\text{HfO}_2,\text{trap}})$, with $\alpha_{e,\text{SiO}_2} = 2(2m_{e,\text{SiO}_2} q\phi_{0,\text{SiO}_2}/\hbar^2)^{0.5}$, and $\alpha_{e,\text{HfO}_2} = 2(2m_{e,\text{HfO}_2} q\phi_{0,\text{HfO}_2}/\hbar^2)^{0.5}$, where m_{e,SiO_2} is $0.95m_0$, m_{e,HfO_2} is $0.03m_0$, $\tau_0 = 6.6 \times 10^{-14}(\text{s})$, d_{SiO_2} is 10 \AA , and $\phi_{0,\text{SiO}_2} = 1.6\text{ eV} + \phi_{0,\text{HfO}_2}$. Finally, it can be acquired that $d_{\text{HfO}_2,\text{trap}}$ is 13 \AA . This is a reasonable value. While V_g transits from $V_{\text{high level}}$ to $V_{\text{base level}}$, electrons in the high- k bulk shallow traps near the gate and substrate discharge to gate and source/drain, respectively. Hence, only traps in the middle of the high- k bulk shallow traps can be measured by the charge pumping technique. In addition, the falling time is $1 \times 10^{-7}(\text{s})$, which matches the time at duty ratio of 98%,

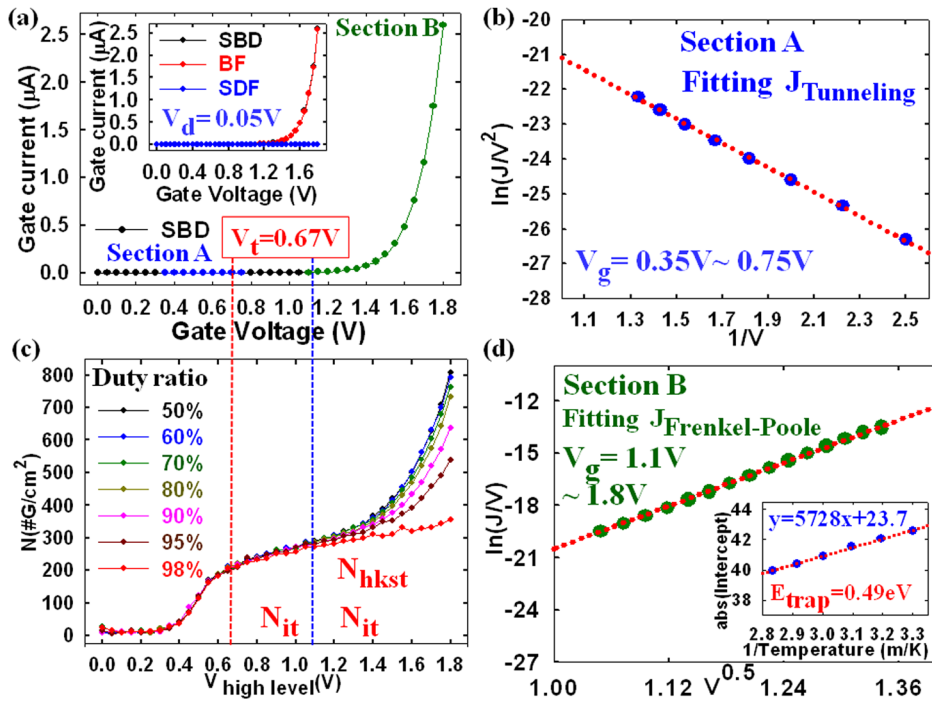


FIG. 3. (a) I_g - V_g characteristic curves with SDB. Inset shows I_g - V_g characteristic curves with BF, SDF, and SDB. (b) Gate current in section A is fitted by tunneling model. (c) N - $V_{high\ level}$ characteristic curves with different duty ratios for charge pumping measurement. (d) Gate current in section B is fitted by Frenkel-Poole model.

that of 1×10^{-7} (s). This implies that electrons in the middle of the high-k bulk shallow traps have no time to tunnel to the substrate in the accumulation area. Thus, only interface traps can be measured by I_{cp} at a duty ratio value of 98%.

Combining the results above, the energy band diagram of the model for charge pumping measurement with anomalous traps can be acquired, as shown in Fig. 4. Figures 4(a) and 4(b) show the energy band diagram when pulses are applied to gate with the charge pumping technique at the high and base levels, respectively. When $1.1\text{ V} > V_{high\ level} > V_t$, gate current is tunneling-path dominated, leading to high-k bulk shallow traps not charging electrons. Electrons merely charge to interface traps, as shown in Fig. 4(a). Subsequently, holes recombine with electrons in the interface

traps at $V_{base\ level}$, as shown in Fig. 4(b). Thus, I_{cp} only detects N_{it} . On the contrary, when $V_g > 1.1\text{ V}$, the gate current is dominated by the Frenkel-Poole mechanism, causing high-k bulk shallow traps to charge electrons. Next, electrons charge in interface traps and high-k bulk shallow traps, as shown in Fig. 4(c). Then holes recombine with electrons in the interface traps at $V_{base\ level}$, and electrons discharge from high-k bulk shallow traps to the body by the tunneling mechanism. Therefore, I_{cp} measures not only interface traps but also high-k bulk shallow traps.

In summary, N - $V_{high\ level}$ characteristic curves are nearly the same in value for $V_{high\ level} < 1.1\text{ V}$ with a rise in duty ratio. However, N decreases with an increase in duty ratio for $V_{high\ level} > 1.1\text{ V}$. This indicates that the electron discharge

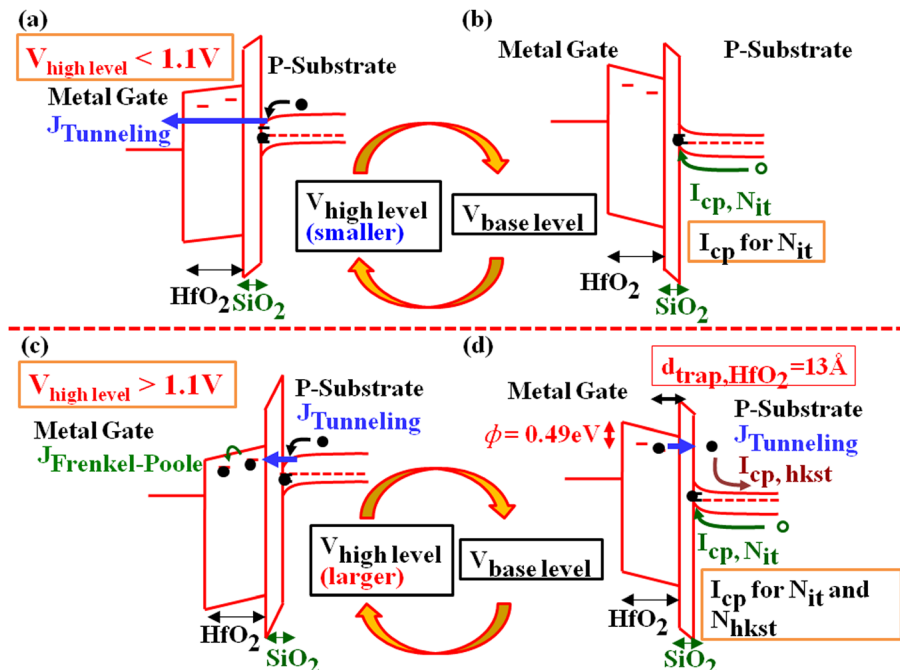


FIG. 4. The energy band diagram of high-k/metal gate MOSFETs with charge pumping measurement (a) in $V_{high\ level}$ and (b) in $V_{base\ level}$, when $V_{high\ level} < 1.1\text{ V}$. The energy band diagram of high-k/metal gate MOSFETs with charge pumping measurement (c) in $V_{high\ level}$ and (d) in $V_{base\ level}$, while $V_{high\ level} > 1.1\text{ V}$.

time dominates the value of N . In addition, the values of e_p obtained by the slope of $\ln(N(t_{\text{base level}} = 2.5 \mu\text{s}) - N(t_{\text{base level}})) - \Delta t_{\text{base level}}$ are independent of temperature. Hence, electrons discharge from high- k bulk shallow traps via the tunneling mechanism. The distance of traps can be acquired by the equation $t = \tau_0 \exp(\alpha_{e,\text{SiO}_2} d_{\text{SiO}_2} + \alpha_{e,\text{HfO}_2} d_{\text{HfO}_2, \text{trap}})$ and $\phi_{0,\text{HfO}_2} = 0.49 \text{ eV}$, and ϕ_{0,HfO_2} can be obtained from fitting the gate current with the Frenkel-Poole mechanism. From this, $d_{\text{HfO}_2, \text{trap}}$ can be calculated to be 13 \AA , a reasonable value. This result is proof that traps are actually located in the high- k shallow bulk. This study shows that anomalous traps measured by the charge pumping technique in a HfO_2 /metal gate at high gate voltage can be attributed to high- k bulk shallow traps.

Part of this work was performed at United Microelectronics Corporation. The work was supported by the National Science Council under Contract No. NSC 101-2120-M-110-002.

¹C. H. Dai, T. C. Chang, A. K. Chu, Y. J. Kuo, S. C. Chen, C. T. Tsai, W. H. Lo, S. H. Ho, G. Xia, O. Cheng, and C. T. Huang, *Surf. Coat. Technol.* **205**, 1470–1474 (2010).

²C. H. Dai, T. C. Chang, A. K. Chu, Y. J. Kuo, F. Y. Jian, W. H. Lo, S. H. Ho, C. E. Chen, W. L. Chung, J. M. Shih, G. Xia, O. Cheng, and C. T. Huang, *IEEE Electron Device Lett.* **32**(7), 847–849 (2011).

³W. H. Lo, T. C. Chang, C. H. Dai, W. L. Chung, C. E. Chen, S. H. Ho, O. Cheng, and C. T. Huang, *IEEE Electron Device Lett.* **33**(3), 303–305 (2012).

⁴Y. J. Kuo, T. C. Chang, P. H. Yeh, S. C. Chen, C. H. Dai, C. H. Chao, T. F. Young, O. Cheng, and C. T. Huang, *Thin Solid Films* **517**, 1715 (2009).

⁵Y. J. Kuo, T. C. Chang, C. H. Dai, S. C. Chen, J. Lu, S. H. Ho, C. H. Chao, T. F. Young, O. Cheng, and C. T. Huang, *Electrochem. Solid-State Lett.* **12**, H32 (2009).

⁶C. H. Dai, T. C. Chang, A. K. Chu, Y. J. Kuo, S. H. Ho, T. Y. Hsieh, W. H. Lo, C. E. Chen, J. M. Shih, W. L. Chung, B. S. Dai, H. M. Chen, G. Xia, O. Cheng, and C. T. Huang, *Appl. Phys. Lett.* **99**, 012106 (2011).

⁷C. H. Dai, T. C. Chang, A. K. Chu, Y. J. Kuo, W. H. Lo, S. H. Ho, C. E. Chen, J. M. Shih, H. M. Chen, B. S. Dai, G. Xia, O. Cheng, and C. T. Huang, *Appl. Phys. Lett.* **98**, 092112 (2011).

⁸C. H. Dai, T. C. Chang, A. K. Chu, Y. J. Kuo, Y. C. Hung, W. H. Lo, S. H. Ho, C. E. Chen, J. M. Shih, W. L. Chung, H. M. Chen, B. S. Dai, T. M. Tsai, G. Xia, O. Cheng, and C. T. Huang, *Thin Solid Films* **520**, 1511 (2011).

⁹W. H. Lo, T. C. Chang, J. Y. Tsai, C. H. Dai, C. E. Chen, S. H. Ho, H. M. Chen, O. Cheng, and C. T. Huang, *Appl. Phys. Lett.* **100**, 152102 (2012).

¹⁰M. B. Zahid, R. Degraeve, M. Cho, L. Pantisano, D. R. Aguado, J. Van Houdt, G. Groeseneken, and M. Jurczak, *IEEE Int. Reliab. Phys. Symp. Proc.* **2009**, 21–25.

¹¹W. J. Zhu and T. P. Ma, *IEEE Electron Device Lett.* **25**(2), 89–91 (2004).

¹²R. Chau, S. Datta, M. Doczy, B. Doyle, J. Kavalieros, and M. Metz, *Electron Devices Lett.* **25**(6), 408–410 (2004).

¹³H. Aozasa, I. Fujiwara, A. Nakamura, and Y. Komatsu, *Jpn. J. Appl. Phys., Part 1* **38**, 1441–1447 (1999).

¹⁴I. Lundström and C. Svensson, *J. Appl. Phys.* **43**, 5045 (1972).

¹⁵T. Wang, N. K. Zous, J. L. Lai, and C. Huang, *IEEE Electron Device Lett.* **19**(11), 411–413 (1998).

¹⁶M. J. Chen and C. Y. Hsu, *IEEE Electron Device Lett.* **33**(4), 468–470 (2012).

¹⁷C. Y. Hsu, H. G. Chang, and M. J. Chen, *IEEE Trans. Electron Devices* **58**(4), 953–959 (2011).

¹⁸C. C. Yeh, T. P. Ma, N. Ramaswamy, N. Rocklein, D. Gealy, T. Graettinger, and K. Min, *Appl. Phys. Lett.* **91**, 113521 (2007).

¹⁹K. Xiong, J. Robertson, M. C. Gibson, and S. J. Clark, *Appl. Phys. Lett.* **87**, 183505 (2005).

²⁰S. H. Ho, T. C. Chang, C. W. Wu, W. H. Lo, C. E. Chen, J. Y. Tsai, H. P. Luo, T. Y. Tseng, O. Cheng, C. T. Huang, and S. M. Sze, *Appl. Phys. Lett.* **101**, 052105 (2012).